



Journal of Materials and Engineering Structures

Research Paper

The Effect of Modified Asphalt Binders by Fourier Transform Infrared Spectroscopy, X-Ray Diffraction, and Scanning Electron Microscopy

Muhammad Mubaraki *

Department of Civil Engineering, Jazan University, King Fahd Road, Jazan, Saudi Arabia

ARTICLE INFO

Article history:

Received : 31 March 2018

Received : 20 December 2018

Accepted : 1 January 2019

Keywords:

asphalt binders

FTIR

X-ray diffraction

Scanning Electron Microscope

ABSTRACT

Two performance-grade asphalt binders, PG 64-10 and PG 76-10, and two modifiers, Acrylate Styrene Acrylonitrile (ASA) polymer and nanomaterials of Al_2O_3 , have been used to modify properties of asphalt mixes. The main function of this study is to characterize and assess materials of modified asphalt binder mixes by three important rheological properties, namely Fourier Transform Infrared Spectroscopy (FTIR), X-ray diffraction (XRD), and Scanning Electron Microscope (SEM). For the same mixes of modified asphalt binders, physical properties were obtained previously, therefore, FTIR, SEM, and XRD results followed the results of physical properties. The data analysis clearly indicates that although the SEM images show uniform dispersion of the ASA and Al_2O_3 , it has been concluded that the FTIR spectra of ASA polymer- and Al_2O_3 -altered asphalt binders were similar notwithstanding highest points, which established that no adjustment in structure occurred in the altered binders associated with the original asphalt binder. The results of the properties of asphalt with the use of ASA polymer are more notable than those with the use of Al_2O_3 nanomaterials.

1 Introduction

The mechanism to find the aging of bituminous binders is tedious work, whereas their physical and macro-mechanical properties are well defined. In [1-2], some sophisticated models have been introduced to understand the rheological and aging performance of bitumen on the macro level. Moreover, there is a research gap of aging impacts analysis on mechanical behavior and its chemical composition, therefore, some studies are investigating this issue. Various methods are presented such as Fourier Transform Infrared Spectroscopy (FTIR), Scanning Electron Microscope (SEM), and X-Ray Diffraction (XRD) are presented to analyze the performance of bituminous binder [3-5]. Among these methods, FTIR is famous in examining oxidizing the aging effects of oxidation on chemical composition, and it provides information about sample absorption of infrared radiation (IR) light, which usually ranges from 400 to 4000 cm^{-1} . Besides, it makes use of the point that bonds in molecules attract IR light at resonant rates that are characteristic for their vibrations. The structure of materials

* Corresponding Author: Tel.: +966 173295000.

E-mail address: mmubaraki@jazanu.edu.sa

is the basis to choose the IR active band, whereas the structure of materials as it comes under the molecular groups. The bituminous binders belong to the carbonyl functional group and the sulfoxide group. These groups are part of the molecular groups. Changes of chemical groups indicate changes in rheological properties. These changes can develop chemomechanical coupling [6, 7].

A comprehensive study of bituminous binder was performed using FTIR, which links chemical structure and mechanical behavior. Under the FTIR analysis, samples were examined for chemical and mechanical tests. A comprehensive analysis of received FTIR spectra is introduced in this paper. This analysis is based on a round-robin study. This study related to bituminous binder is unable to signify sensitive methods to analyze FTIR spectra, while it is the most reproducible of all significant approaches. Moreover, enhancing reproducibility, the effect of short-term aging temperature on oxidative acceptance during short- and long-term aging was examined. The acceptance of oxidation is measured by changing carbonyl ($C=O$) and sulfoxide ($S=O$) bands [8].

Besides the FTIR method, a Scanning Electron Microscope (SEM) method has potential to find the structure of asphalt binder. SEM is a microscopic technique where a narrowly carefully focused electron beam is used to clarify the area of observation. It identifies the various properties of a sample from the signals of secondary electrons and backscatter electrons. Secondary electrons are electrons that are liberated from their energy level by an electron beam. They are very sensitive to surface topography and can be used to obtain images of the specimen. Backscattered electrons are beam electrons that have been scattered back toward the surface of the specimen, and they are less sensitive to topography. However, it is important to note that the electron microprobe has detection limits which differ for each element and are generally affected by the overall composition of the specimen and the analytical conditions [9-13].

The XRD is a nondestructive method and is one of the principal techniques that provide information about the macrostructure and crystallite parameters of asphalt mixtures, degree thickness of thin films and multi-layers, and defined atomic arrangement [14]. Two-phase admixtures are limited by 3%, while drop up to 0.1% using synchronous radiation. XRD technique has been extensively used to examine and compare crystalline parameters. Alternatively, aromaticity of asphaltenes is achieved from both fresh and aged asphalt in Saudi Arabia, RasTanura (RT), and Kuwait (KW) refineries. The performance of both types of asphaltenes has been estimated and compared using XRD techniques. XRD has seen significant variations in structure and aging patterns in both types of asphaltenes. The results show that the main reason of aging behavior and its components of asphalt are both the source and chemistry. Rolling thin-film oven tests and pressurized aging vessel tests have been used to simulate asphalt aging in this research [15].

In a study, XRD patterns are found by means of monochromatic Cu-K-a radiation at 40kV and 40mA on Rigaku D Max 2200V-PC for twenty-three samples of asphalt binder that were obtained from different locations in North America. The outcomes of the 23 samples of asphalt binder were obtained by XRD on thin films. It shows two factors which relate reasonably well with aging tendency at low temperature. Analysis and understanding of structural and compositional properties of asphalt binders at the microscopic level are expected to enhance the performance and durability of asphalt pavements [16].

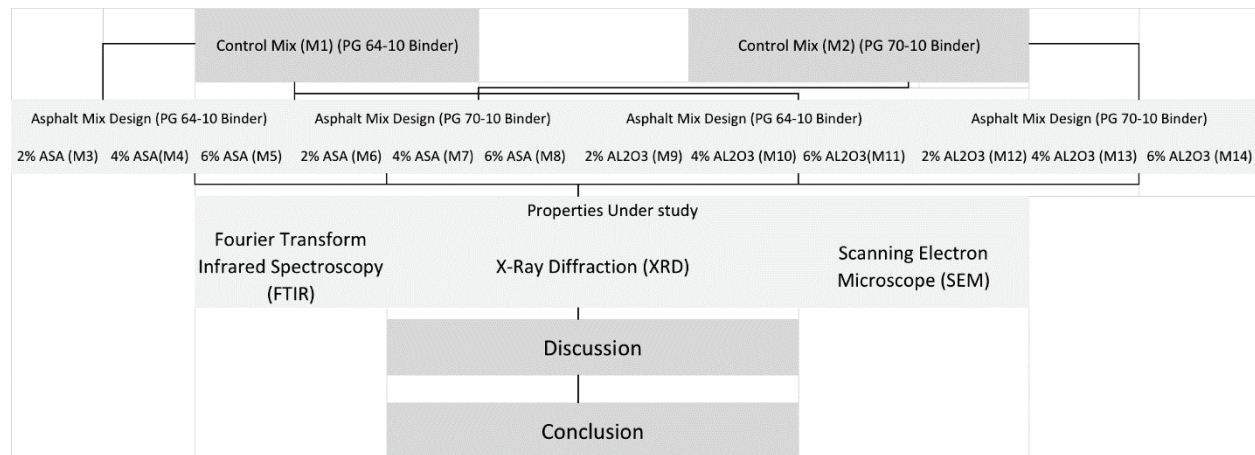
To conclude, the aim of the present study is to use previous results about some characteristics of asphalt binders including physical properties, conducted by the same author of this study. The performance of physical properties, when ASA polymer and nanomaterials of Al_2O_3 were added, is functioned for the current study with analysis of FTIR Spectroscopy, XRD, and SEM of asphalt mixes having unlike proportions of ASA and Al_2O_3 .

2 Materials and Methods

Modified asphalt binders PG 64-10 and PG 70-10, with a penetration of 68 and 69 mm at 25°C, respectively, ductility of 104 and 105 cm, respectively, and a softening point of 49.3 and 51.7°C, respectively, were used for all mixtures in the study. Samples were made by means of the dissolve mixing method by enhancing different percentage contents by weight of ASA polymer or Al_2O_3 nanomaterial to the base. The asphalt was heated until it transformed into fluid form. A Silverson high-shear mixer was used for the mixing method, which was carried out at 170°C ($\pm 1^\circ C$) and a speed of 5000 rpm for one and a half hours. The results of viscosity, stability, complex of modulus, rutting, and fatigue were obtained previously, and Table 1 shows the results according to research done previously [17]. The following subsections highlight the methodology of FTIR, XRD, and SEM. Figure 1 displays the flow chart of the study.

Table 1 –Properties of base asphalt binders and modified asphalt binders [17]

Properties of unmodified and modified asphalt binders											
Asphalt Binders (The Control Mixes)	Penetration, mm			Softening point °C			Ductility, cm				
	PG 64-10	PG 70-10	PG 64-10	PG 70-10	PG 64-10	PG 70-10	PG 64-10	PG 70-10	PG 64-10	PG 70-10	PG 64-10
	68	69	49.3	51.7	104	105					
Modified Asphalt Binder at Different Percentages (%)	PG 64-10	PG 70-10	PG 64-10	PG 70-10	PG 64-10	PG 70-10	ASA	Al ₂ O ₃	ASA	Al ₂ O ₃	ASA
2	59	64	48	59	48	51	50	51	51	103	53
4	55	63	22	54	50	49	56	53	40	100	41
6	54	61	36	54	52	48	53	51	35	97	35
											91

**Fig. 1 –Flow Chart of the Study**

2.1 Fourier Transform Infrared Spectroscopy(FTIR)

Macromolecular materials are such materials as polymer-modified asphalt binders (PMA) and nanomaterial-modified asphalt (NMA). The Perkin Elmer spectrometer Model 400 was used for all composites with wavenumbers ranging between 650 cm⁻¹ and 4000 at room temperature. Functional groups with one, two, and three chemical bonds have to be determined or specified between the carbon and other groups of mixed modified asphalt according to correlation tables. The intensity and the position determine the characteristics of functional groups as summarized in correlation tables [16, 18].

Absorption and wavenumber are two important parameters in the analysis of FTIR spectra. For example, absorption spectroscopy works as a tool in analytical chemistry to define the existence of a detailed material in a sample and, in some situations, to compute the quantity of the material remaining. The function of the frequency explains the variation in the intensity of the absorption which can be realized in the absorption continuum. The frequencies and their related intensities primarily change in the electronic and molecular configuration of the sample. The frequencies will also change in the relations among particles in the sample, the crystal configuration in the solids, and in some environmental causes such as temperature and pressure [19].

2.2 X-Ray Diffraction (XRD)

Examining and comparing the crystal and the microstructure of base asphalt concrete and the modified asphalt binders at different absorptions of Al_2O_3 nanomaterials and ASA polymer can be achieved by the method of X-Ray Diffraction (XRD). DSR sample molds at a thickness of 2 mm were used to control the tests fixed at room temperature (25°C). Software called Bruker AXS D4 Endeavor was used in this study, which helps enable understanding of the asphalt materials' microstructure and to deliver data on the crystalline parameters of layer diameter, interlamellar distance, number of lamellar, height of the unit cell, and aromaticity. These deliverables data are useful in understanding the behavior of the cracking and helping in setting necessary maintenance [15–23].

2.3 Scanning Electron Microscope (SEM)

Micrographs of the asphalt mixtures were captured using a scanning electron microscope (SEM). SEM is a method to evaluate the dispersion of added materials such as ASA and Al_2O_3 and to ensure uniformity of dispersion within the matrix of the asphalt binder. Specimens were cut into small pieces of approximately ($20 \times 20 \times 10$) mm for testing, and the samples were then coated with a gold/palladium alloy to increase the stiffness at the surface and to obtain conductivity without affecting observed surface morphology, in order to make them relatively more stable during the testing. The interior structure of the asphalt binder is changed upon the introduction of modifiers [22, 23].

3 Results and Discussion

3.1 Transform Infrared Spectroscopy (FTIR) investigations

Samples of PG 64-10 containing 0, 2, 4, and 6% of ASA polymer or Al_2O_3 nanomaterial were subjected to Fourier Transform Infrared Spectroscopy (FTIR) investigations. After mixing the asphalt binder with ASA polymer or nanomaterials of Al_2O_3 , the functional groups are presented in Figure 2 for both ASA and Al_2O_3 .

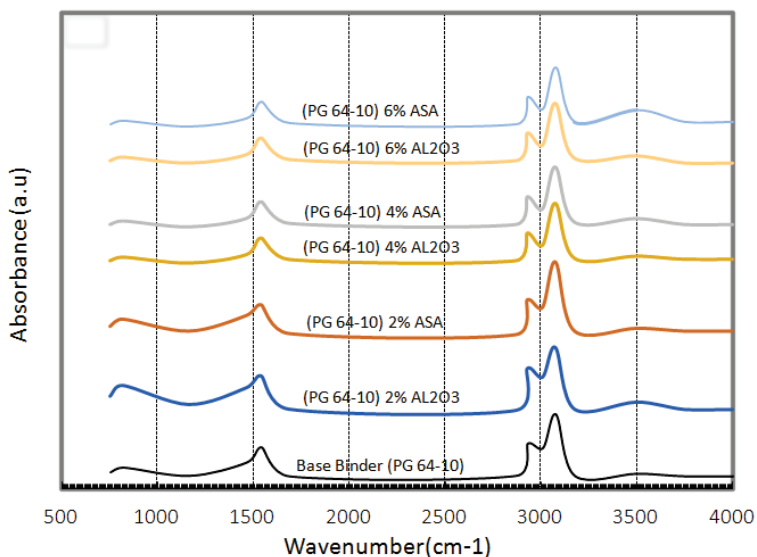


Fig. 2–FTIR Spectrum results for Base and Modified PG64-10

For FTIR spectra of the base, the O-H groups have no peak at wavenumbers of more than 3150 cm^{-1} , which means there was no retention of water in the samples. Moreover, two wide-ranging points were detected in the $2928.00 - 3076.52 \text{ cm}^{-1}$ array, which could be allocated for the C-H group that forms aliphatic chains. In addition, the comparison of peak position and intensities of various peaks appearing in the FTIR spectra of the base, and in the modified mixtures with either ASA or Al_2O_3 , reveal that the relative intensity of the peaks appears in the region of $3000 - 3150 \text{ cm}^{-1}$. Groups of C-C do not have strong absorption at the wavenumber of 1686.92 cm^{-1} which denotes aromatic compounds. Likewise, a smaller peak was found at 1462.96 and 1542.90 cm^{-1} because of spreading vibrations of the C-H from CH_3 , and S-O spreading vibrations were found at 1163.77 cm^{-1} . Lastly, the highest at the range between $753.36 - 819.62 \text{ cm}^{-1}$ was recognized to be benzene,

because of the spreading vibration of the C–H bond. The sulphoxide bonds S–O spreading vibrations were identified at 1163.77 cm⁻¹.

Instead, the FTIR spectra of ASA and Al₂O₃ in PG 64-10 samples were similar for all peak points, as seen in Figure 2, which established that no variation in the structure of the modified binders associated with the base binder was attained. The concentrations of ASA / Al₂O₃ samples (2–6%) dropped to the pure sample of base asphalt, with asphalt molecules positively happened and enriched other features [16].

Comparably with the PG 64-10 results, the FTIR spectra for the base of asphalt binder PG 70-10 samples, and also for the modified asphalt binder samples mixed with the nanomaterials of Al₂O₃ and the polymer ASA at different percentages (2, 4, and 6%), are presented in Figure 3. The functional groups are presented in Figure 3 for both ASA and Al₂O₃. However, Figure 3 includes the observation that the O–H groups have no peak at wavenumbers more than 3500 cm⁻¹, different than 3150 cm⁻¹ when PG 64-10 was used, which means there was no retention of water in the samples. All other groups are very similar in peak ranges compared to modified PG 64-10. In terms of comparison, the peak position and intensities of various peaks appearing in the FTIR spectra of the base, and in the modified binder PG 64-10, reveal that no peaks appear after 3150 cm⁻¹, while the FTIR of modified PG 70-10 has no peaks after 3500 cm⁻¹. This indicates that the free O–H group of polymeric species undergoes some interactions with asphalt binders.

Furthermore, to conclude, carbonyl bonds, (C–O) butadiene double bonds (HC=CH), and sulphoxide bonds (S–O) were exposed for marginally changing ranges of base and ASA / Al₂O₃ which typically centered at 1686.92 cm⁻¹, 966.1 and 1163.77 cm⁻¹ respectively. HC=CH and S–O associated with C–O from the base sample have revealed a rise in the modified samples. The outcomes display asphalt with no clear alterations before and after adaptation, which shows that indicates that a change in asphalt with Al₂O₃ nanomaterial or ASA polymer is purely a physical process.

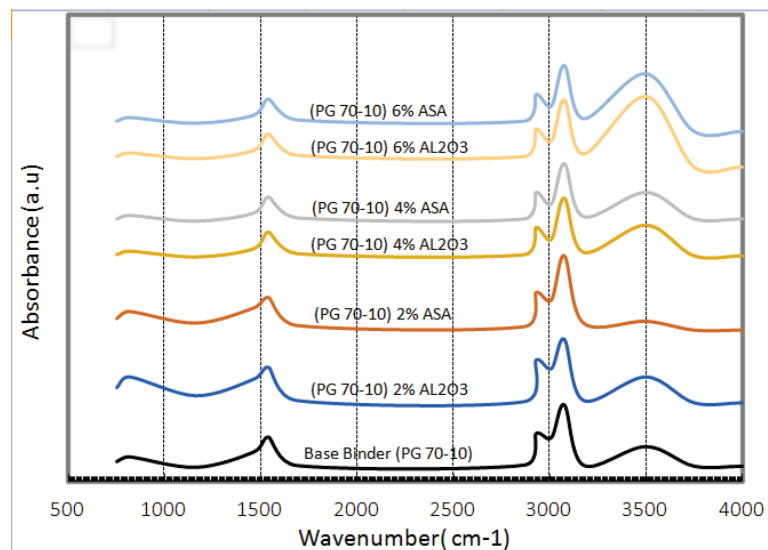


Fig. 3—FTIR Spectrum Results for Base and Modified PG70-10

3.2 X-ray diffraction analysis

XRD analysis was directed to examine the modifications in structural features of base binder and asphalt binder improved by ASA polymer and Al₂O₃ nanomaterials. The proportion of the crystalline phase was quantified by means of dedicated software for both ASA and Al₂O₃. Bruker AXS, D8 Advance was the software used for the research. The base asphalt binder was absolutely without any defined peaks, which means the asphalt binder was not crystallized, as shown in Figure 4. The alteration of the binder samples consisting of 2, 4, and 6% concentrations of ASA polymer and Al₂O₃ nanomaterials deviate the stage of the mixtures of asphalt and the modifiers. Furthermore, a different wide-range of consideration at a low angle shows a semi-crystalline phase of the ASA and Al₂O₃ adapted asphalt. It is acknowledged that raising the absorption of the ASA polymer raises the proportion of the crystalline phase. However, after adding Al₂O₃ nanomaterials, it was found that all of the binders are still to some extent amorphous to the original asphalt binder in the different absorptions of 2, 4, and 6%.

For example, at 2% of ASA, the proportion of the crystalline phase has been boosted by 3.23 %, while at 4% of ASA, the proportion of the crystalline phase has been boosted to a value of 5.08 %, which represents the highest among the three percentages of ASA. In contrast, for 6% of ASA, a drop in the quantity of the crystalline phase is witnessed. However, these observations have not generally been made when nanomaterials of Al_2O_3 were added. For example, at 4% of Al_2O_3 , the proportion of the crystalline phase was not the same as when % ASA polymers were added. This result, concludes that the addition of 4% of both ASA and Al_2O_3 yields the highest values of the crystalline phase with consideration that the pattern of different percentages of Al_2O_3 is not the same pattern as that of different percentages of ASA. This implies that the distribution of Al_2O_3 nanomaterials in the binders was arbitrary. But the outcomes clearly show that the ASA polymer has a significantly greater consequence on the arrangement of asphalt than does the Al_2O_3 . Furthermore, measuring the alterations in the structure of the improved binders requires that the measurement of the crystalline stage can be indicated by means of dedicated software to ensure uniformity in the matrix.

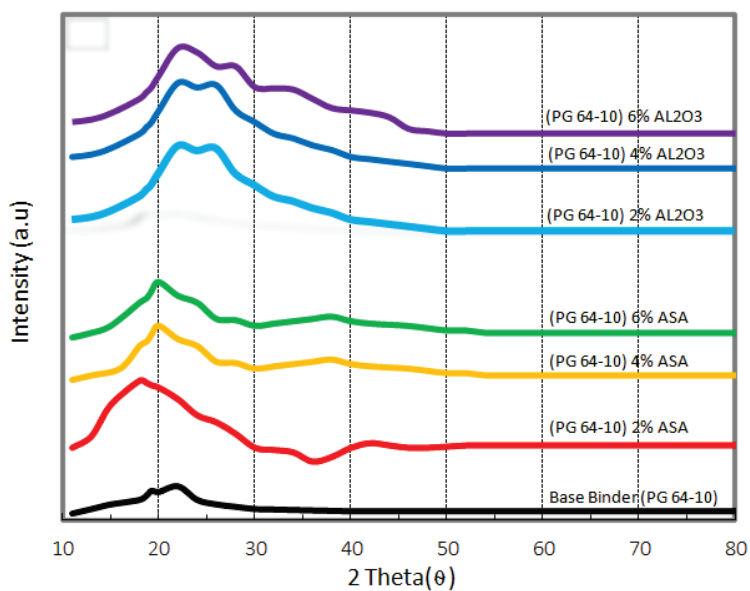


Fig. 4–XRD Results for Base and Modified PG64-10

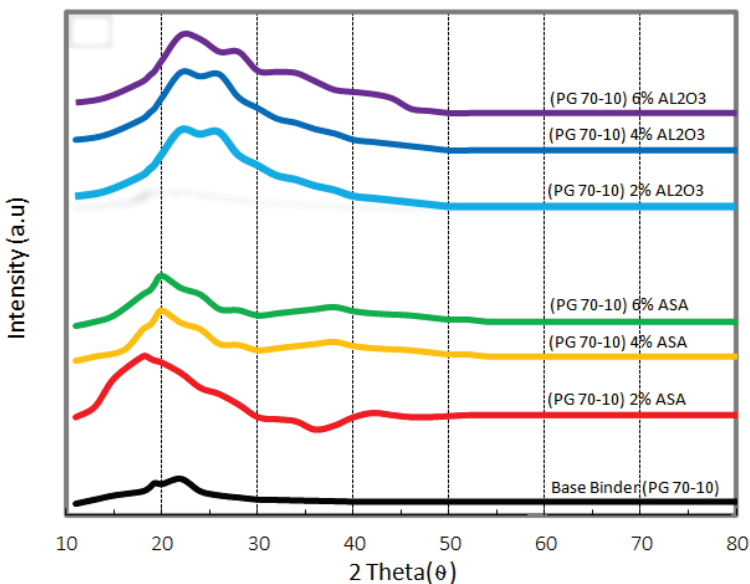


Fig. 5–XRD Results for Base and Modified PG70-10

Figure 5 displays the outcomes attained for the base asphalt binder PG 70-10 and the different percentages of added Al_2O_3 and ASA to that base binder. For example, at 2% of ASA, the proportion of the crystalline phase has increased by 3.89

%, while at 4% of ASA, the proportion of the crystalline phase has increased to a value of 5.63 %. At 6% it decreased. XRD investigation was directed in order to examine the variations in the structural features of asphalt binder mixed with ASA polymer and Al_2O_3 nanomaterials. It is evident in Figure 5 that the nanomaterials have a semi-crystal-like structure.

3.3 Scanning Electron Microscope (SEM)

Images obtained by use of the scanning electron microscopic (SEM) are shown in Figures 6 and 7 for both asphalt binders at different concentrations. The SEM images of ASA polymer- and Al_2O_3 nanomaterials-modified asphalt binders are useful in recognizing the deviations in the microstructure of the adapted asphalt binders, as well as in showing the dispersion of the modifiers. However, the accuracy of the images is questionable [23].

The plain structure of the base asphalt binder is shown in Figures 6a and 7a. It is likely that a few Al_2O_3 particles dispersed in the asphalt. The modified base asphalt binders by Al_2O_3 and ASA polymer structure are also shown in Figure 6b through 6g and 7b through 7g. Both nanomaterials and the polymer material reacted with asphalt and were intercalated and exfoliated. Some group particles were still scattered in the asphalt matrix. Intercalated structure was shown as well as the interaction between the modified material and the asphalt.

It was observed in Figure 6 a, b, and c that the distribution of ASA polymer in the binder matrix was uniform. This is due to the low melting temperature, resulting in a homogeneous binder. Figure 6 e, f, and g shows the SEM for Al_2O_3 nanomaterials-modified asphalt binders at 2, 4, and 6%, respectively. The difference in structure between the modified and base asphalt showed the possibility of chemical reactions between asphalt and nanomaterials and polymers. Nanomaterials were scattered homogenously in the asphalt matrix.

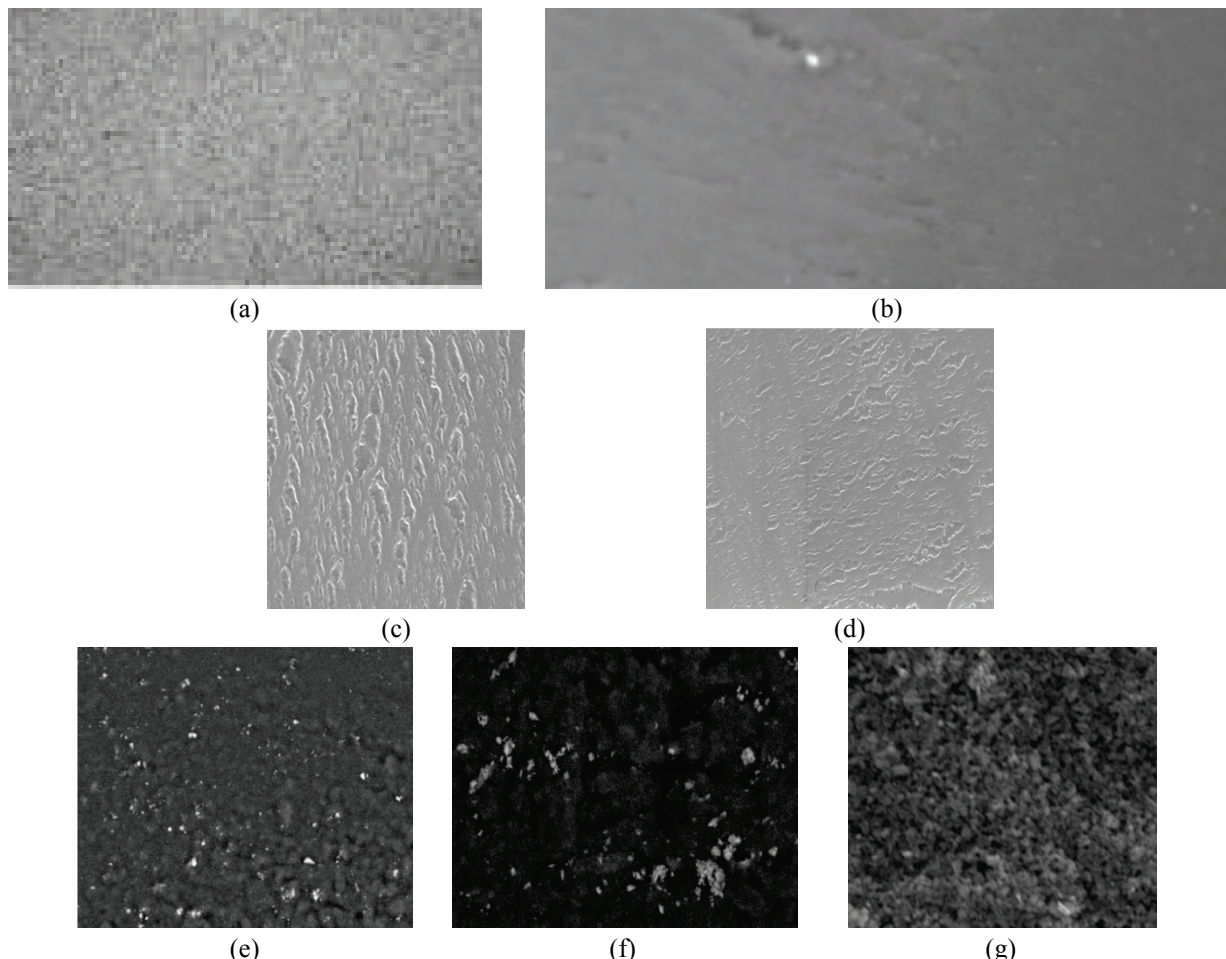


Fig.6 - SEM Images of Asphalt Binder PG 64-10 with (a) Base, (b) 2%ASA, (c) 4%ASA, (d) 6% ASA, (e) 2% Al_2O_3 , (f) 4% Al_2O_3 , and (g) 6% Al_2O_3

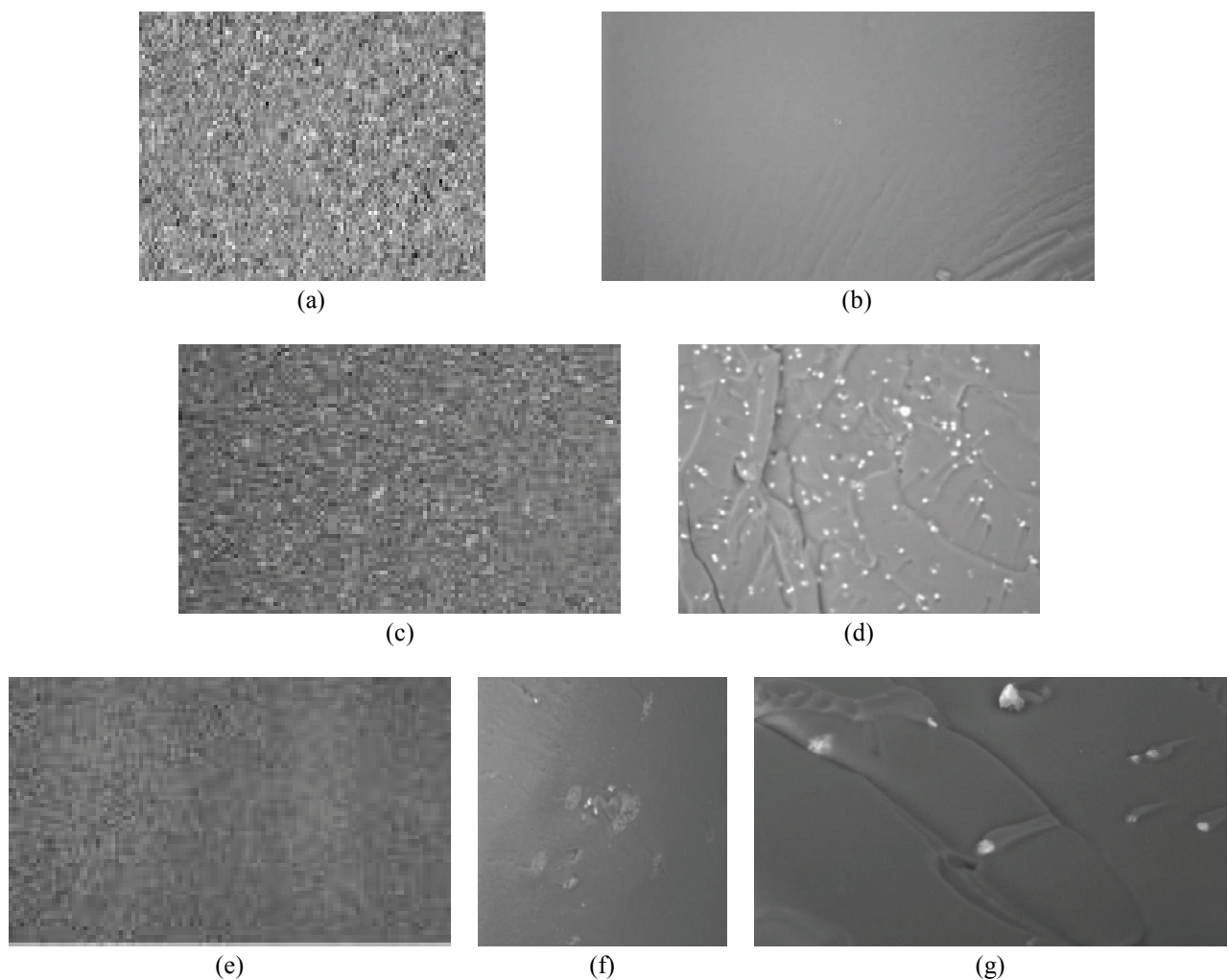


Fig. 7 - SEM Images of Asphalt Binder PG 70-10 with (a) Base, (b) 2%ASA, (c) 4%ASA, (d) 6% ASA, (e) 2% Al_2O_3 , (f) 4% Al_2O_3 , and (g) 6% Al_2O_3

4 Conclusions

The innovation claimed in this paper can be seen in the light of previous studies. Fourier Transform Infrared Spectroscopy (FTIR), X-ray Diffraction (XRD), and Scanning Electron Microscope (SEM) have been investigated in this study with the help of results on physical properties of asphalt mixes containing ASA and Al_2O_3 obtained previously. However, ASA polymer and Al_2O_3 had not been used as extensively as other materials, in other research. The comparison between the two materials under study was clearly expressed as the research assessed the material properties of asphalt binder modified with ASA polymer and Al_2O_3 nanomaterials. This study was with respect to rheological properties at high temperatures in terms of FTIR, XRD, and SEM using results of the same author's previous research. The resulting points can be stated based on the attained outcomes:

The modified asphalt binders can be sustained in storage at high temperatures, particularly modified asphalt binder containing Al_2O_3 nanomaterials, while binder with ASA polymer can be sustainably stored up to 4% ASA content.

The FTIR spectra of ASA polymer- and Al_2O_3 -altered asphalt binders remained similar despite highest points, which established that no adjustment in structure occurred in the altered binders associated with the original asphalt binder.

The XRD results show that raising the absorption of the ASA polymer raises the part of the crystalline phase. However, after adding nanomaterials of Al_2O_3 , it was found that all of the binders are still to some extent amorphous to the original asphalt binder in the different absorptions of 2, 4, and 6%.

The SEM results show that both nanomaterials and the polymer material reacted with asphalt and were intercalated and exfoliated. Some group particles were still scattered in the asphalt matrix. Intercalated structure was shown as well as the interaction between the modified material and the asphalt.

Generally, the adjustment of asphalt binder using ASA polymer and Al₂O₃ nanomaterials has a significant influence on the physical properties of the asphalt binder. The samples changed with Al₂O₃ nanomaterials display better-improved outcomes than the samples modified with ASA polymer. The amount of 4% can well be considered the ideal quantity for both modifiers.

Acknowledgements

The author would like to acknowledge the assistance he received from Jazan Municipality and the College of Engineering of Jazan University, where the author used the lab facilities to conduct some of the lab work. Their assistance and support made the production of this paper possible.

REFERENCES

- [1]- M. Costanzi, D. Cebon, Generalized phenomenological model for the viscoelasticity of bitumen. *J. Eng Mech.* 141(5) (2015) 339-410. doi:10.1061/(ASCE)EM.1943-7889.0000835
- [2]- L. Eberhardsteiner, J. Füssl, B. Hofko, F. Handle, M. Hospodka, R. Blab, H. Grothe, Towards a microstructural model of bitumen aging behaviour. *Int. J. Pavement Eng.* 16(10) (2015) 939-949. doi: 10.1080/10298436.2014.993192
- [3]- Y.S. Kumbargeri, K.P. Biligiri, Rational performance indicators to evaluate asphalt materials' aging characteristics. *J. Mater. Civil Eng.* 28(12) (2016) 04016157. doi:10.1061/(Asce) Mt. 1943-5533.0001681
- [4]- M.R. Nivitha, E. Prasad, J.M. Krishnan, Ageing in modified bitumen using FTIR spectroscopy. *Int. J. Pavement Eng.* 17(7) (2016) 565-577. doi:10.1080/10298436.2015.1007230
- [5]- J.C. Petersen, R. Glaser, Asphalt oxidation mechanisms and the role of oxidation products on age hardening revisited. *Road Mater. Pavement* 12(4) (2011) 795-819. doi:10.1080/14680629.2011.9713895
- [6]- Z.G. Feng, S.J. Wang, H.J. Bian, QL. Guo, XJ. Li, FTIR and rheology analysis of aging on different ultraviolet absorber modified bitumens. *Constr. Build. Mater.* 115 (2016) 48-53. doi :10.1016/j.conbuildmat.2016.04.040
- [7]- B. Hofko, M.Z. Alavi, H. Grothe, D. Jones, J. Harvey, Repeatability and sensitivity of FTIR ATR spectral analysis methods for bituminous binders. *Mater. Struct.* 50(3) (2017) 187. doi:10.1617/s11527-017-1059-x
- [8]- B. Hofko. L. Porot. A. Falchetto Cannone. L. Poulikakos. L. Huber. X. Lu. K. Mollenhauer. H. Grothe, FTIR spectral analysis of bituminous binders: reproducibility and impact of ageing temperature. *Mater. Struct.* 51(2) (2018) 45. doi :10.1617/s11527-018-1170-7
- [9]- J. Goldstein, D.E. Newbury, P. Echlin, D.C. Joy, Jr Roming, A.D. Lyman, C.E. Fiori, E. Lifshin, Scanning Electron Microscopy and X-Ray Microanalysis: A Text for Biologists, Materials Scientists, and Geologists. Springer US, second Edition, 1992.
- [10]- P.K. Das, H. Baaj, S. Tighe, N. Kringos, Atomic force microscopy to investigate asphalt binders: a state-of-the-art review. *Road Mater. Pavement* 17(3) (2016) 693-718. doi: 10.1080/14680629.2015.1114012
- [11]- S.H. Firoozifar, S. Foroutan, S. Foroutan, The effect of asphaltene on thermal properties of bitumen. *Chem. Eng. Res. Des.* 89(10) (2011) 2044-2048. doi:10.1016/j.cherd.2011.01.025
- [12]- Q. Qin, M.J. Farrar, A.T. Pauli, J.J. Adams, Morphology, thermal analysis and rheology of Sasobit modified warm mix asphalt binders. *Fuel*. 115 (2014) 416-425. doi:10.1016/j.fuel.2013.07.033.
- [13]- K. Gebresellasie, Investigation of asphalt binders by X-Ray Diffraction using Pearson-VII, Pesudo-Voigt and Generalized Fermi Functions, Master Thesis, Memorial University of Newfoundland, 2012
- [14]- M.N. Siddiqui, M. Farhat Ali, J. Shirokoff, Use of X-ray diffraction in assessing the aging pattern of asphalt fractions. *Fuel* 81(1) (2002) 51-58. doi:10.1016/S0016-2361(01)00116-8
- [15]- S.I. Albrka Ali, A. Ismail, M.R. Karim, N.I.M. Yusoff, R.A. Al-Mansob, E. Aburkaba, Performance evaluation of Al₂O₃ nanoparticle-modified asphalt binder. *Road Mater. Pavement* 18(6) (2017) 1251-1268. doi:10.1080/14680629.2016.1208621
- [16]- H.E.-D M. Sallam, M. Mubarak, N.I.M. Yusoff, Application of the Maximum Undamaged Defect Size (d max) Concept in Fiber-Reinforced Concrete Pavements. *Arab. J. Sci. Eng.* 39(12) (2014) 8499-8506.

doi:10.1007/s13369-014-1400-4

- [17]- M. Mubaraki, Comparison of Laboratory Performance of Two Superpave Binders Mixed with Two Modifiers. *Road Mater. Pavement* (2018) In Press. doi:10.1080/14680629.2018.1541138
- [18]- M. Mubaraki, Maintenance strategies at project level for low volume urban roads. *Int. J. Pavement Res. Technol.* 5(4) (2012) 225-233. doi:10.6135/ijprt.org.tw/2012.5(4).225
- [19]- M.M. Ba-Abbad, P.V. Chai, M.S. Takriff, A. Benamor, A.W. Mohammad, Optimization of nickel oxide nanoparticle synthesis through the sol-gel method using Box-Behnken design. *Mater. Des.* 86(2015) 948-956. doi:10.1016/j.matdes.2015.07.176
- [20]- M.E. Jacox, Vibrational and electronic energy levels of polyatomic transient molecules: supplement B. *J. Phys. Chem. Ref. Data* 32(1) (2003) 321-441. doi:10.1063/1.1497629
- [21]- J. Michael Hollas, *Modern Spectroscopy*. John Wiley & Sons, Inc. Fourth Edition, 2004.
- [22]- B. Glaoui, M. Merbouh, M. Van De Ven, E. Chailloux, A. Youcef, How thermal fatigue Cycles change the rheological behavior of polymer modified bitumen?. *Energy Procedia* 36 (2013) 844-851. doi:10.1016/j.egypro.2013.07.097
- [23]- H. Viet Vo, D.W. Park, Application of conductive materials to asphalt pavement. *Adv. Mater. Sci. Eng.* Article ID 4101503 (2017). doi:10.1155/2017/4101503